Angewandte
International Edition Chemie

DOI: 10.1002/anie.201208685

Chirality Transfer

Chirality Transfer in a Methyl Lactate–Ammonia Complex Observed by Matrix-Isolation Vibrational Circular Dichroism Spectroscopy**

*Christian Merten and Yunjie Xu**

Vibrational circular dichroism (VCD) spectroscopy[1] has become a powerful tool for the determination of the absolute configurations of natural products,[2] metal complexes,[3] and synthetic materials, such as drugs[4] and polymers.[5] It has also attracted much attention in biochemical research,[6] for example, very recently in studies of the formation of insulin fibrils.[7] Its unique sensitivity to chirality and conformational changes makes it a desirable tool for studies of self-aggregation or solute–solvent interactions involving chiral molecules.[8] An interesting, but not yet fully understood, type of solute–solvent interaction results in the transfer of chiral information to solvent molecules. For example, VCD bands arising from vibrational modes of achiral solvent molecules have been observed for water in a handful of examples in solution;[9] the "chiral imprint" of a chiral solute on the surrounding solvent molecules has been used to explain the drastically different optical rotation dispersion values observed in different solvents.[10]

The combination of VCD spectroscopy and the matrix-isolation (MI) technique has some very attractive advantages and offers opportunities to probe unusual species that are not possible in solution. Although its proof-of-concept was reported in the 1980s,[11] very few results have subsequently been reported. This is mainly due to the stringent requirements on the quality of the matrices prepared, as VCD signal intensity is typically in the range of 10^{-4}–10^{-5} of its parent IR absorption intensity. With technical advances in both VCD and MI spectroscopy, there has been renewed interest in this powerful combination.[12] Trapping a molecule or molecular cluster of interest in a cold rare-gas matrix yields bands with much narrower line width, and allows for spectroscopic studies without the influence of solvent environments and under more controlled sample compositions. Hence, MI-VCD spectroscopy makes it possible to observe bands that might be too broad in solution-phase experiments. It also facilitates unambiguous band assignments and therefore a more reliable determination of the contribution of different conformers to the observed experimental spectra as it was shown recently for 3-butyn-2-ol.[13]

Herein, we describe the first experimental VCD study on the transfer of chirality from a chiral molecule, methyl lactate (ML), to a gaseous species, ammonia. The absorbance bands of ammonia are found in the mid-infrared region from 3500–3200 cm^{-1} (N−H stretching), 1680–1600 cm^{-1} (N−H bending), to 1050–950 cm^{-1} (deformation).[14] The N−H bending modes of ammonia are ideal for the observation of possible chirality transfer from interaction with a chiral molecule, such as ML. These experiments can only be conducted under MI-VCD conditions, as ammonia deprotonates ML in aqueous solution.

To ensure a high level of confidence in the experimental spectra of the ML$\cdots$NH$_3$ complex, the MI-VCD spectrum of ML was studied first to allow a comparison with the spectrum of the complex. Figure 1 shows the experimental MI-IR and VCD spectra obtained for both enantiomers of ML in an argon matrix at a deposition temperature of 10 K. The MI-IR spectrum agrees well with a previous matrix study.[15] The MI-VCD spectra of the two enantiomers show good mirror images and narrow bands, thus allowing a detailed comparison with the calculated spectra. The previous matrix study of ML established that only two of the three theoretically predicted lowest-energy conformations (Supporting Information, Figure S2) contribute to the spectrum at 10 K with contributions of approximately 95 % and 5 %.[15] At 10 K, the

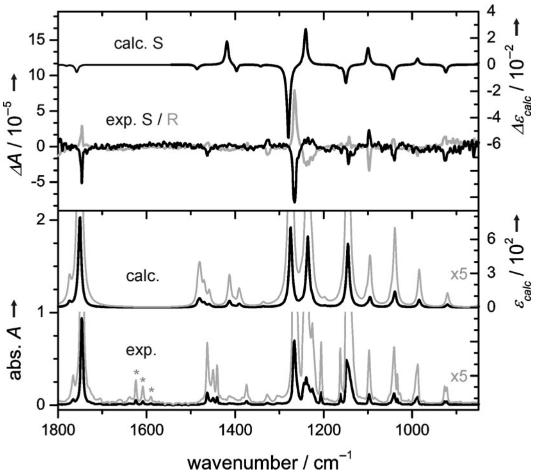

Figure 1. Comparison of the experimental MI-IR and VCD spectra of ML at 10 K with the calculated spectra. A detailed band assignment is given in the Supporting Information, Figure S1. The bands of residual water in the matrix are marked with an asterisk.

---

[*] Dr. C. Merten, Prof. Dr. Y. Xu
Department of Chemistry, University of Alberta
Edmonton, AB, T6G2G2 (Canada)
E-mail: yunjie.xu@ualberta.ca

[**] This research was funded by the University of Alberta and the Natural Sciences and Engineering Research Council of Canada. C.M. thanks the Alexander von Humboldt foundation for a Feodor Lynen postdoctoral fellowship. We gratefully acknowledge access to the computing facilities provided by the Western Canadian Research Grid (Westgrid). Y.X. holds a Tier I Canada Research Chair in Chirality and Chirality Recognition.

Supporting information for this article is available on the WWW under http://dx.doi.org/10.1002/anie.201208685.

third conformer is expected to convert into the second-lowest energy structure, with a low conversion barrier of about 0.5 kcal mol^{-1}. The experimental and calculated spectra, especially of the VCD spectra, show excellent correlation. Only the C−H rocking vibration, which is experimentally observed at 1328 cm^{-1}, was predicted with the wrong VCD sign. The predicted strong positive VCD band for the in-plane C-O-H bending vibration at 1418 cm^{-1} agrees well with the experimental band at 1414 cm^{-1}, which is actually very broad and therefore weaker in intensity. Furthermore, the C−O$_{ester}$ stretching vibration at 1224 cm^{-1} shows site splitting, which was also observed in the previous IR matrix study.[15] Such site splitting does not alter the VCD sign of this mode. In other words, every site-split IR band has the same VCD sign. Further details on the structures, energies, normal mode analysis, and band assignments, as well as the IR and VCD spectra of the individual ML conformers can be found in the Supporting Information.

Owing to the very weak VCD signal intensity (Figure 1), it is important for MI-VCD studies that the absorbance bands of the species of interest are strong enough in the VA spectrum. Therefore, to find the right deposition conditions that yield enough ML···NH$_3$ clusters, various mixing ratios of ML/NH$_3$ have been evaluated. The ratios varied from 1:2 to 1:5, diluted in argon with ML/Ar ratios of 1:500 to 1:860. Furthermore, depositions were carried out at both 10 K and 30 K, which allowed a certain degree of annealing of the matrix and diffusion of the small NH$_3$ molecules during the deposition. In general, it has been found that the dilution of the mixture of ML and NH$_3$ with argon does not significantly affect the observed VA spectra. In the 10 K depositions, the ML/NH$_3$ ratio mostly affected the IR spectral pattern, with bands originating from NH$_3$ and larger pure NH$_3$ clusters because of its simultaneous hydrogen bonding donor and acceptor capabilities,[14] whereas the associated VCD pattern remained essentially unchanged. This suggests little formation of the ML···NH$_3$ clusters at 10 K. The deposition temperature has been found to be the key parameter influencing the formation of the ML···NH$_3$ clusters. Depositions at 30 K yielded a significantly different spectral pattern in the VA spectrum, with the ML/NH$_3$ ratio being a control parameter for the amount of the ML···NH$_3$ clusters formed. It should be noted that the VA spectrum of pure ML does not change upon increasing the deposition temperature to 30 K. This indicates that little self-aggregation takes place under the chosen conditions.

For the previously evaluated 1:3 and 1:5 mixtures, the MI-VCD spectra were recorded for both enantiomers of ML. In Figure 2, the obtained MI-IR and MI-VCD spectra of both enantiomers, which show very good mirror images, are compared with those of pure ML. As the amount of ammonia is increased, there are some characteristic spectral changes, which indicate the formation of the ML···NH$_3$ clusters. For example, a new band appears at 1755 cm^{-1}, the higher wavenumber side of the carbonyl vibration centered at 1746 cm^{-1} in pure ML. The corresponding changes are also visible in the related VCD spectra. More significant changes are observed in the 1400–1200 cm^{-1} region, as indicated in Figure 2. The in-plane O−H bending band at 1262 cm^{-1}, which dominates the IR and VCD spectrum of pure ML, decreases until it becomes very small compared to the surrounding VA and VCD bands in the 1:5 mixtures. At the same time, the new VCD bands at 1296 and 1211 cm^{-1} appear in the spectra of the mixtures. There are other obvious spectral changes with the addition of NH$_3$, for example, new strong VA bands of pure NH$_3$ and of the related clusters in the 1650–1600 cm^{-1} and 1100–1000 cm^{-1} regions.[14] Owing to the strong absorbance bands in the latter region, the noise level in the corresponding region of the MI-VCD spectra has increased. Careful examination of the 1650–1600 cm^{-1} region reveals some new weak VCD bands in the spectra of the 1:3 and 1:5 mixtures, which do not belong to pure ML. These small VCD bands indicate transfer of chirality from methyl lactate to ammonia, making these measurements the first example of chirality transfer from a chiral molecule to an achiral gaseous molecule.

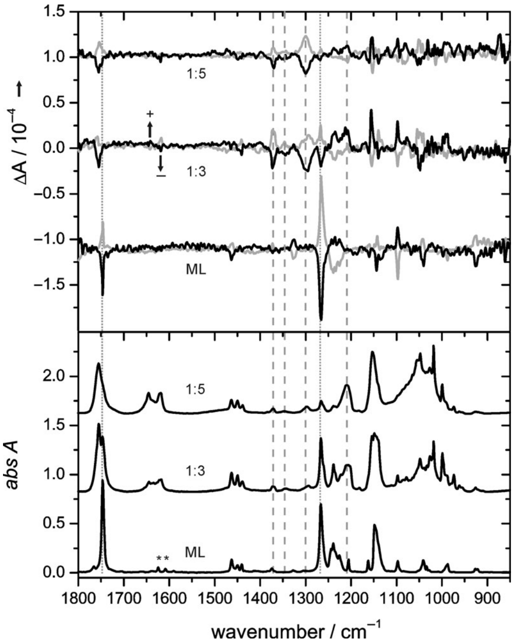

Figure 2. Comparison of the MI-IR and MI-VCD spectra of pure ML (obtained at 10 K) with the spectra obtained for the 1:3 and 1:5 ML/NH$_3$ mixtures at 30 K. The bands of residual water in the matrix are marked with an asterisk. The dotted and dashed lines inidicate characteristic bands of the ML monomer and the ML···NH$_3$ complex, respectively, which change with the sample composition.

To further interpret the experimental data, spectral calculations for the ML···NH$_3$ complex have been carried out. Based on the three most stable conformations found for ML (Supporting Information, Figure S1),[15,16] four structures of the ML···NH$_3$ complex can be generated. Based on the most stable ML conformer, which features an intramolecular hydrogen-bonded ring, two insertion conformations were obtained (Figure 3). In both conformers, the ammonia molecule inserts into the intramolecular hydrogen bonded ring. The main structural difference between the two conformers is the OCCO angle, which is about −33.5° in conformer 1 and +6° in conformer 2. The OH-group orientation is adjusted to keep intact the two hydrogen bonds

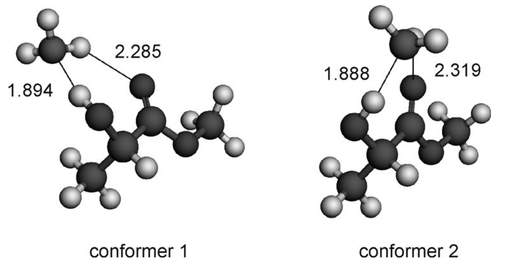

Figure 3. Geometries of the two most stable conformers of ML$\cdots$NH$_3$.

formed by the inserted ammonia. The structures feature a zero-point corrected energy difference (ΔE) of 0.15 kcal mol^{-1}, favoring conformer 1. The other two conformers are more than 2 kcal mol^{-1} less stable. A potential energy surface scan indicates an interconversion energy barrier of about 1.4 kcal mol^{-1} from conformer 1 to conformer 2. For details on the structures, relative energies, and interconversion barrier see the Supporting Information, Figures S4–S6.

Theoretical IR and VCD spectra of ML$\cdots$NH$_3$ have been calculated for all four conformers (Figure S7). If one assumes a Boltzmann distribution of the ML$\cdots$NH$_3$ conformers at 30 K, conformer 1 has 92.6% of the population, whereas conformer 2 has only 7.4%. This results in an unsatisfying agreement between the experimental and theoretical VCD spectra (for a detailed comparison of the single conformer spectra with the experimental ones, see Figure S8). Clearly, contributions from both ML$\cdots$NH$_3$ conformers 1 and 2 are vital. The two most stable pure ML conformers were determined to have about 95% and 5% population in an Ar matrix.[15] Assuming a kinetically controlled formation of ML$\cdots$NH$_3$ at 30 K, the two low-energy insertion conformers, that is, conformers 1 and 2, would each contribute 47.5%, whereas the third conformer contributes 5%. In Figure 4, the population-weighted theoretical spectra are compared with the experimental spectra obtained for the 1:5 mixtures. In general, the calculation predicts the VCD spectrum of the complex to be weaker in intensity than that of pure ML. This is consistent with the experimental observation. As can be seen in Figure 4, both the IR and VCD features observed can be clearly correlated to the calculated ones of the ML$\cdots$NH$_3$ complex. Based on the normal mode analyses provided in the Supporting Information, there are three VA bands that can be identified as arising almost solely from the ammonia vibrations in ML$\cdots$NH$_3$. These are the N–H bending vibrations between 1700–1600 cm^{-1} and the NH$_3$ deformation mode at 1080 cm^{-1} (indicated in Figure 4). In the experimental VCD spectra, the calculated positive VCD band for this deformation mode seems to correlate with the experimental VCD spectral feature. This can be seen as further evidence for the occurrence of chirality transfer from ML to ammonia. The calculated VCD pattern for the N–H bending region agrees only partially with the experimentally observed pattern. These VCD bands are weak in both experiment and calculation. And the theoretically predicted VCD signs for some of the bands may be incorrect (for a robust mode analysis, see the Supporting Information).[17]

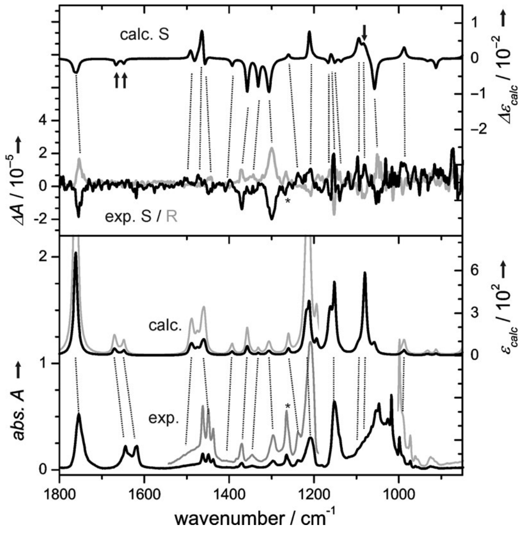

Figure 4. Comparison of the MI-IR and MI-VCD spectra of the 1:5 mixtures of ML/NH$_3$ (obtained at 30 K) with the calculated spectra of ML$\cdots$NH$_3$. The arrows mark the three ammonia vibration modes discussed in the text. The asterisk marks the only remaining visible band of pure ML in the 1:5 mixtures (1262 cm^{-1}).

The proposed kinetically controlled formation of the molecular complex in the matrix based on the ML monomer populations seems reasonable. The predeposited 1:5 gas mixture contains almost exclusively free ML and NH$_3$ molecules. A deposition at 10 K freezes this gas phase situation, with trace amount of NH$_3$ dimer,[14] whereas the matrix is soft enough to allow the diffusion of small NH$_3$ molecules in the 30 K deposition. Each of them either meets another NH$_3$ molecule or approaches a ML monomer. The conformation distribution of the ML monomer is then preserved when the ML$\cdots$NH$_3$ complex is formed.

In conclusion, we have presented the first MI-VCD study on the interaction of a chiral molecule, methyl lactate, and an achiral gaseous molecule, ammonia. Although the VCD intensity is four to five orders of magnitude smaller than the infrared, one can detect VCD signals of the complexes reliably with a high-quality cold rare gas matrix. With the experiments and calculations presented herein, we have shown that chirality can be transferred from ML to NH$_3$ through hydrogen bonding interactions. The fact that these measurements would not be possible in solution further highlights the power of MI-VCD spectroscopy in studying exotic chiral molecular complexes and chirality transfer phenomena.

Experimental Section

Both enantiomers of ML were purchased from Sigma Aldrich and NH$_3$ was obtained from Scott speciality gases, Inc. Prior to deposition, the ML samples were degassed by a repeated freeze-pump-thaw procedure. Mixtures of ML/NH$_3$/Ar were prepared by standard manometric techniques. The matrix system consists of a closed-cycle helium cryostat from Advanced Research Systems, Inc. (ARS 4HW compressor with DE 204SI expander) and a stainless steel vacuum line. The flow of the gas mixture to a cold window (BaF$_2$) was held constant at 1.5 sccm (sccm = standard cubic centimeters per minute) using a flow controller (MKS 1179A).

The IR and VCD spectra were recorded with a Bruker Vertex 70 equipped with a PMA 50 module for polarization modulated measurements. All spectra were recorded with a spectral resolution of 2 cm^{-1}. The MI-VCD spectra were averaged over at least 30000 scans.

The Gaussian09 program package[18] was used to perform the geometry optimizations and harmonic spectra calculations at the B3LYP/6-311++G(2d,p) level of theory. The IR and VCD spectra were simulated by assigning a Lorentzian line shape with a half-width at half-height of 4 cm^{-1} to the calculated dipole and rotational strength. The calculated harmonic frequencies were scaled by 0.994 for better comparison with the experimental spectra.

Received: October 29, 2012

Keywords: chirality transfer · density functional calculations · hydrogen bonding · matrix isolation · vibrational circular dichroism

[1] a) L. A. Nafie, *Vibrational Optical Activity*, Wiley, Chichester, **2011**; b) G. Yang, Y. Xu, *Top. Curr. Chem.* **2011**, *298*, 189–236; c) Y. He, W. Bo, R. K. Dukor, L. A. Nafie, *Appl. Spectrosc.* **2011**, *65*, 699–723.

[2] a) E. Burgueño-Tapia, C. M. C. García-Rojas, P. Joseph-Nathan, *Phytochemistry* **2012**, *74*, 190–195; b) J. M. Batista, A. N. L. Batista, J. S. Mota, Q. B. Cass, M. J. Kato, V. S. Bolzani, T. B. Freedman, S. N. Lopez, M. Furlan, L. A. Nafie, *J. Org. Chem.* **2011**, *76*, 2603–2612.

[3] a) H. Sato, H. Uno, H. Nakano, *Dalton Trans.* **2011**, *40*, 1332–1337; b) H. Sato, R. Takase, Y. Mori, A. Yamagishi, *Dalton Trans.* **2011**, *40*, 0; c) C. Merten, K. Hiller, Y. Xu, *Phys. Chem. Chem. Phys.* **2012**, *14*, 12884–12891.

[4] a) T. B. Freedman, R. K. Dukor, P. J. C. M. van Hoof, E. R. Kellenbach, L. A. Nafie, *Helv. Chim. Acta* **2002**, *85*, 1160–1165; b) D. Dunmire, T. B. Freedman, L. A. Nafie, C. Aeschlimann, J. G. Gerber, J. Gal, *Chirality* **2005**, *17*, 101–108.

[5] a) C. Merten, A. Hartwig, *Macromolecules* **2010**, *43*, 8373–8378; b) H.-Z. Tang, E. R. Garland, B. M. Novak, J. He, P. L. Polavarapu, F. C. Sun, S. S. Sheiko, *Macromolecules* **2007**, *40*, 3575–3580.

[6] a) V. Andrushchenko, Z. Leonenko, D. Cramb, H. van de Sande, H. Wieser, *Biopolymers* **2002**, *61*, 243–260; b) V. Andrushchenko, D. Tsankov, H. Wieser, *J. Mol. Struct.* **2003**, *661–662*, 541–560.

[7] a) D. Kurouski, R. K. Dukor, X. Lu, L. A. Nafie, I. K. Lednev, *Biophys. J.* **2012**, *103*, 522–531; b) D. Kurouski, R. K. Dukor, X. Lu, L. A. Nafie, I. K. Lednev, *Chem. Commun.* **2012**, *48*, 2837–2839.

[8] a) C. Merten, M. Amkreutz, A. Hartwig, *Phys. Chem. Chem. Phys.* **2010**, *12*, 11635–11641; b) V. P. Nicu, E. J. Baerends, P. L. Polavarapu, *J. Phys. Chem. A* **2012**, *116*, 8366–8373; c) Y. Liu, G. Yang, M. Losada, Y. Xu, *J. Chem. Phys.* **2010**, *132*, 234513.

[9] a) M. Losada, P. Nguyen, Y. Xu, *J. Phys. Chem. A* **2008**, *112*, 5621–5627; b) M. Losada, H. Tran, Y. Xu, *J. Chem. Phys.* **2008**, *128*, 014508; c) M. Losada, Y. Xu, *Phys. Chem. Chem. Phys.* **2007**, *9*, 3127–3135; d) G. Yang, Y. Xu, *J. Chem. Phys.* **2009**, *130*, 164506; e) J. Sadlej, J. C. Dobrowolski, J. E. Rode, *Chem. Soc. Rev.* **2010**, *39*, 1478–1488.

[10] a) P. Mukhopadhyay, G. Zuber, P. Wipf, D. N. Beratan, *Angew. Chem.* **2007**, *119*, 6570–6572; b) P. Mukhopadhyay, P. Wipf, D. N. Beratan, *Acc. Chem. Res.* **2009**, *42*, 809–819.

[11] a) D. W. Schlosser, F. Devlin, K. Jalkanen, P. J. Stephens, *Chem. Phys. Lett.* **1982**, *88*, 286–291; b) D. Henderson, P. L. Polavarapu, *J. Am. Chem. Soc.* **1986**, *108*, 7110–7111.

[12] a) G. Tarczay, G. Magyarfalvi, E. Vass, *Angew. Chem.* **2006**, *118*, 1807–1809; *Angew. Chem. Int. Ed.* **2006**, *45*, 1775–1777; b) S. Góbi, E. Vass, G. Magyarfalvi, G. Tarczay, *Phys. Chem. Chem. Phys.* **2011**, *13*, 13972–13984.

[13] C. Merten, Y. Xu, *ChemPhysChem* **2013**, *14*, 213–219.

[14] S. Süzer, L. Andrews, *J. Chem. Phys.* **1987**, *87*, 5131–5139.

[15] A. Borba, A. Gómez-Zavaglia, L. Lapinski, R. Fausto, *Vib. Spectrosc.* **2004**, *36*, 79–88.

[16] a) P. Ottaviani, B. Velino, W. Caminati, *Chem. Phys. Lett.* **2006**, *428*, 236–240; b) N. Borho, Y. Xu, *Phys. Chem. Chem. Phys.* **2007**, *9*, 1324–1328.

[17] a) V. P. Nicu, E. J. Baerends, *Phys. Chem. Chem. Phys.* **2009**, *11*, 6107–6118; b) V. P. Nicu, E. J. Baerends, *Phys. Chem. Chem. Phys.* **2011**, *13*, 16126–16129; c) S. Góbi, G. Magyarfalvi, *Phys. Chem. Chem. Phys.* **2011**, *13*, 16130–16133; d) V. P. Nicu, J. Neugebauer, E. J. Baerends, *J. Phys. Chem. A* **2008**, *112*, 6978–6991.

[18] Gaussian09 (Revision C.01): M. J. Frisch et al.; see the Supporting Information for full reference.